RESEARCH ARTICLE

Predicting Factors of Safety for Soil Slope Stability Based on Various Slope Characteristics and Rainfall Conditions

Tan Yi Xuan[1] · Aniza Ibrahim[1*] · Fakhrurazi Awang Kechik[1] · Aizat Mohd Taib[2] · Dayang Zulaika Abang Hasbollah[3] · Mohd. Firdaus Md Dan@Azlan[4] ·

[1]Department of Civil Engineering. Faculty of Engineering, Universiti Pertahanan Nasional Malaysia, Kem Sungai Besi, 57000, Wilayah Persekutuan Kuala Lumpur, Malaysia.

[2]Department of Civil Engineering, Faculty of Engineering and Built Environment, Universiti Kebangsaan Malaysia, 43600, Bangi, Selangor, Malaysia.

[3]Centre of Tropical Geoengineering, Universiti Teknologi Malaysia, 81300, Skudai, Johor, Malaysia.

[4]Sustainable Geostructure & Underground Exploration, Faculty of Civil Engineering & Built Environment, Universiti Tun Hussein Onn Malaysia, 86400 Batu Pahat, Johor, Malaysia.

*corresponding author email: aniza@upnm.edu.my

Abstract

The occurrence of rainfall has resulted in multiple instances of slope failure in the Klang Valley region of Malaysia. Bukit Antarabangsa, located in the Ampang District of Selangor, Malaysia, has been prone to frequent slope collapses for a long time. However, the specific elements, apart from rainfall, that contribute to landslides in the area have not yet been discovered. The objective of this study is to examine the effects of varying degrees of rainfall intensity and duration on distinct land formations to enhance the understanding of the complex mechanism of landslides at Bukit Antarabangsa. This study has chosen three locations each in Bukit Antarabangsa and Universiti Pertahanan Nasional Malasyia (UPNM) campus area for the purpose of collecting samples and conducting tests. The laboratory conducted an examination of both disturbed and undisturbed soil samples to assess the soil's fundamental and hydraulic properties. This analysis included evaluating the soil's sieve analysis, Atterberg limits, shear strength, falling head permeability, and pressure plate extractor. The results are employed for numerical simulation in the SEEP/W and SLOPE/W modules of the Geostudio software. Parametric studies are performed on different slope configurations, including slope angle, height, and piezometric line, during rainfall periods extending two and eight hours. The real-time intensity of rainfall is tracked by monitoring the rainfall intensity at the closest rainfall station for the purpose of simulation. A factor of safety (FoS) was determined for each individual scenario. The numerical simulation results indicate that slope failure occurs when the shear strength of the soil decreases with an increase in soil moisture content due to a decrease in soil suction. The soil samples exhibit variations in matric suction, hydraulic conductivity, effective internal friction angle, and effective cohesion. The hydraulic and mechanical properties of each soil sample influence its slope safety factor, even when subjected to similar slope conditions in simulations.

Keywords Rainfall-induced landslide · Unsaturated soil · Slope characteristics · Factor of Safety · Numerical Simulation

Introduction

A landslide, also known as a slope failure, is a geohazard occurrence characterised by a movement of soil surface, rock falls, or a combination of both caused by gravitational forces, as stated by Batterson, M. et al. (1999). Landslides are a geological occurrence where masses of earth and rockslide down a slope. They are a common form of natural hazard experienced globally (Ray 2021). Slope stability refers to the ability of soil or rock slopes to withstand or undergo movement. As a result, slope instability leads to slope failure. Landslides pose a significant risk to the safety of individuals and their property in tropical countries such as Indonesia, Malaysia, Singapore, and Thailand (Alsubal et al. 2019). In inland, coastal, and marine environments, rockfalls can cause slope failures or shallow discharge floods. Large-scale soil movements serve as an indication that these phenomena are currently taking place (Cruden 1991). Rainfall, toe erosion, and sudden fluctuations in the water table commonly cause landslides. Landslides are considered a geo-environmental catastrophe with significant risks due to their severe negative impacts on society and the economy (Abeykoon 2018; Abeykoon 2019; Baum 2010; Petley 2012). Other than economic reason, landslide also can have a significant influence on the health, and safety of the residents, particularly in Malaysia, a country that has witnessed numerous slope failures in the past as a result of rainfall (Razali 2023).

Peninsular Malaysia experiences a significant number of landslides annually, with a particular concentration in the Kuala Lumpur and Selangor areas. The extensive growth of cities has made the Hulu Kelang region in Gombak, Selangor, very prone to landslides (Zulkafli 2021). Multiple building and development projects in this hilly terrain have necessitated the construction of platforms and excavation work on the slopes of the hills (Huat 2012). Consequently, the geotechnical instability causes landslides, leading to mortality in some cases. The collapse of Highland Towers in Taman Hillview, Hulu Kelang, marked the most devastating landslide in Malaysia's history, claiming the lives of 48 individuals on December 11, 1993. Similarly, Taman Bukit Mewah in Bukit Antarabangsa, Hulu Kelang, experienced the second catastrophic landslide in the region, resulting in the loss of five lives and significant damage to 14 bungalow units on December 6, 2008. Notably, this incident occurred a mere 1.4 kilometres away from Highland Tower (Zulkafli 2021). The Hulu Kelang region has witnessed several notable landslide incidents caused by rainfall. On May 15, 1999, a landslide closed the only access route to the residential area, causing concern for over 10,000 residents of Bukit Antarabangsa. Other landslides occurred at Taman Zooview on October 29, 2001, and November 8, 2001; Taman Hillview on November 20, 2002, resulting in eight casualties and the destruction of one bungalow; and Kampung Pasir on May 31, 2006, resulting in four casualties and damage to three longhouses. On December 16, 2022, a catastrophic landslide took place at Father's Organic Farm in Batang Kali, Hulu Selangor, Selangor, resulting in the second-highest number of casualties since the fall of Highland Towers. A total of 31 individuals lost their lives in this tragic incident. Furthermore, Kuala Lumpur is prone to landslides, with a total of 50 incidents documented in the city region between 2010 and 2020 (Zulkafli 2021).

Geology, lithology, hydrology, and morphology, along with other physical elements, have the potential to impact landslides (Kazmi 2016; Cerri 2017). Landslides occur with greater frequency in regions characterised by intricate geological conditions (Yi 2021; Xia 2021). The landslide that caused the collapse of Highland Towers was due to the demolition of retaining walls, inadequate drainage and designs of cut and fill slopes surrounding the tower, all of which occurred during continuous heavy rainfall. The Taman Bukit Mewah landslide occurred

due to an excessive buildup of pore-water pressure in the slope, as documented by Low (2012) and Al-Karni (2011).

Various factors, such as extended and intense rainfall, earthquakes, volcanic eruptions, topography, soil properties, changes in groundwater levels, disturbances, and modifications in slope profile due to construction activities, or a combination of these factors, can influence or trigger landslides (Rahman 2017; Qasim 2013; Jamaludin 2012). Landslides can also be caused by other factors, such as improper application of prescribed procedures, insufficient study of past failures, and design deficiencies such as inadequate site-specific ground investigation (Rahman 2017). Furthermore, a contributing factor to landslides is the failure to account for water movement, as seen by the failure to accurately assess the ability of surface drainage and current groundwater levels. Despite Malaysia not being a mountainous country and having less than 25% of its topography covered by mountains and hills, slope failures or landslides nonetheless occur in the country (Qasim 2013).

Hence, precipitation is a significant contributing element to the occurrence of landslides or slope failures (Liu 2021; Kechik 2023). The intensity and pattern of rainfall affect the occurrence of landslides (Li 2021). Precipitation and seepage greatly impact the soil properties (Pajalić 2021). According to Lee (2009) rainfall infiltration reduces soil matric suction, resulting in a decrease in its shear strength and an increase in the possibility of slope failures (Gallage 2021; Huang 2021; Ibrahim 2018). When the pore-air pressure is lower than the pore-water pressure, it is called matric suction (Kristo 2019). An increase in matric suction leads to a decrease in the volumetric water content of the soil, as observed in the soil-water characteristic curve (SWCC) (Kristo 2019). The development of matric suction creates tension forces on the soil particles at the air/water interface, which enhances the soil's shear strength (Kristo 2019; Hou 2021; Ibrahim 2013). Di (2021) and Xiao (2021) have found that rainfall can lead to the formation of a perched water table, an elevation in the main groundwater level, surface erosion, and a rise in the unit weight of soil due to a surge in moisture content. Other than that it was shown that slopes with a greater gradient heavier rainfall, and soils with larger particles all led to an increase in the amount of sediment (Liu 2021).

Furthermore, several factors significantly influence the stability of a slope, including slope geometry, soil qualities (such as physical, mechanical, and hydraulic characteristics), initial moisture content, groundwater level, intensity and length of rainfall, and intermittent rainfall. These variables can be utilised in the development of an early warning system for slope failures, with the aim of minimising losses caused by slope disasters.

Shallow landslides are the most common type in Malaysia. Normally, typically occur after or immediately following heavy rains and have a slide surface that is less than four meters deep have observed various types of landslides, including deep-seated slides, debris flows, and geologically controlled failures like wedge failure and rock fall (Ting 1984). Following several instances of rainfall, continuous low-intensity precipitation will elevate the groundwater level, leading to a profound landslide (Han 2014). Studies by Tsai (2008), Tsaparas (2002), Collins (2004), Tohari (2007) and Chen (2004) have identified rainfall as a prominent catalyst for landslides.

Malaysia experiences a high frequency of landslide accidents due to its yearly tropical rainfall and the transitional monsoon, which occurs twice a year from November to March and from May to September Suhaila (2010) and Pour (2015). As a result of the geographic setting of the mid-latitude region near the equator, there has been an excess of tropical rainfall throughout the monsoon season, whether in the form of prolonged rainfall or short intense downpour, which has triggered the initial stages of shallow landslides (Maturidi 2021). In the meantime, if there is persistent antecedent rainfall for several days or weeks or occasional excessive rainfall, landslides can also happen in April and October during the inter-monsoon season. According to a report by the

Malaysian Department of Irrigation and Drainage (DID) in 2018, Malaysia had an average yearly rainfall of 3,000 mm throughout the period from 2013 to 2017 (Maturidi 2021). The mean yearly precipitation in Peninsular Malaysia's west coast regions ranges from 1,700 millimetres to 2,100 millimetres, which is significantly lower than that of the east coast regions, including Terengganu and Kelantan. In 2017, the east coast experienced annual rainfall between 2,900 millimetres and 3,600 millimetres. As a result, the entire region experiences shallow landslides due to the significant annual precipitation.

Many studies have focused on examining the relationship between various factors and slope failure. The studies, however, only examine a limited number of soil characteristics that could potentially cause slope failure. For example, Gallage (2021) examined the impact of slope inclination on the occurrence of slope failures triggered by rainfall. At three distinct slope inclinations of 30, 45, and 60 degrees, a simulated downpour was applied to three instrumented model box experiments. The experiments continued until the slope collapsed. The soil-based model slopes were homogeneous since they were comprised of just one type of soil, which was Edosaki soil, and were only subjected to 40 mm/hr of rainfall. The goal of the instrumented model slopes was not to accurately replicate the slope's actual conditions. The instrumented model slopes were therefore not designed to represent the actual conditions of the slope. Similarly, Kristo (2019) used numerical modelling to investigate the effects of several rainfall events on a naturally occurring slope in the Paima region of the Bajura district in Nepal. In this research, just one type of soil, poorly graded sands, was studied using a geometrical model with a slope length of 400 metres, a slope angle of 25°, a soil depth of ten-metre, and a groundwater level of eight-metre from the surface.

In a similar manner, Zhang (2022) employed a numerical model featuring a ten-metre slope height, a slope angle of 45 degrees, and an initial groundwater level of three metres to examine the impact of different types of rainfall on the onset of slope collapse. The models executed 5808 iterations, encompassing 11 unique categories of soil attributes across 528 predetermined combinations of rainfall intensity and duration (I-D). Nevertheless, this study primarily focused on analysing two specific types of soil: Toyoura sand and volcanic soil. On the other hand, Kazmi (2016) looked at how suction changes the calculated factor of safety (FoS) of slopes made of unsaturated soil by measuring its shear strength and unit weight. A parametric study was undertaken by varying the height of the slope to 5, 10, and 15 metres and adjusting its angle to 25, 30, 35, 40, 45, 50, 55, 60, 65, 70, 75, and 80 degrees. Three sorts of common soils, namely sandy soil, silty soil, and clayey soil were utilised to analyse the stability of the slope. Nevertheless, this analysis did not consider either the precipitation volume or the groundwater level. Other than that, review from Wong (2022), examines the impact of climate change on slope stability, with a particular focus on the influence of environmental elements like precipitation, temperature fluctuations, and extreme weather occurrences. The study synthesises evidence from various geographies and approaches to emphasise the complex influence of climate change on slope failures and landslides. Other than that study by Marrapu (2021) use artificial neural networks (ANN) to forecast slope stability and assess the significance of various contributing elements. The study highlights the utilisation of innovative computational methods to improve the comprehension and forecasting of slope stability through the examination of various geotechnical and environmental elements.

Peninsular Malaysia was formed by diverse geological structures with a variety of soil types; therefore, it is obvious that a single or limited range of soil types cannot effectively represent the actual slope conditions in a specific place. In addition, Malaysia experiences a tropical rainforest environment characterised by high

temperatures, excessive humidity, and frequent rainfall. Malaysia has a consistent occurrence of rainy weather throughout the year.

This study will examine the fluctuations in the intensity and duration of rainfall. Furthermore, no studies have demonstrated the correlation between several characteristics, including those previously mentioned, and the matric suctions of different soil types, as well as slope stability. To demonstrate, one can examine the correlation between the angle of a slope and the matric suctions of different unsaturated soil types under specific rainfall I-Ds and groundwater levels, or vice versa, by keeping the slope height constant. This study will ultimately examine the combined impact of these characteristics on slope stability and aim to assess the influence of matric suction on the stability of unsaturated soils during rainfall-induced slope instability. It considers a variety of factors, including slope height, slope angle, soil mechanical and hydraulic properties, groundwater level, and rainfall intensity and duration.

Materials and Methods

Soil Sampling and preparation

For this study, a total of six soil samples were examined. The soil samples were obtained from two main locations: Universiti Pertahanan Nasional Malaysia (UPNM), Sungai Besi, Kuala Lumpur; and Bukit Antarabangsa, Hulu Kelang, Selangor, as depicted in **Fig. 1**. The three soil samples were acquired from UPNM (A, B and C), while the other three (D, E and F) were gathered from Bukit Antarabangsa.

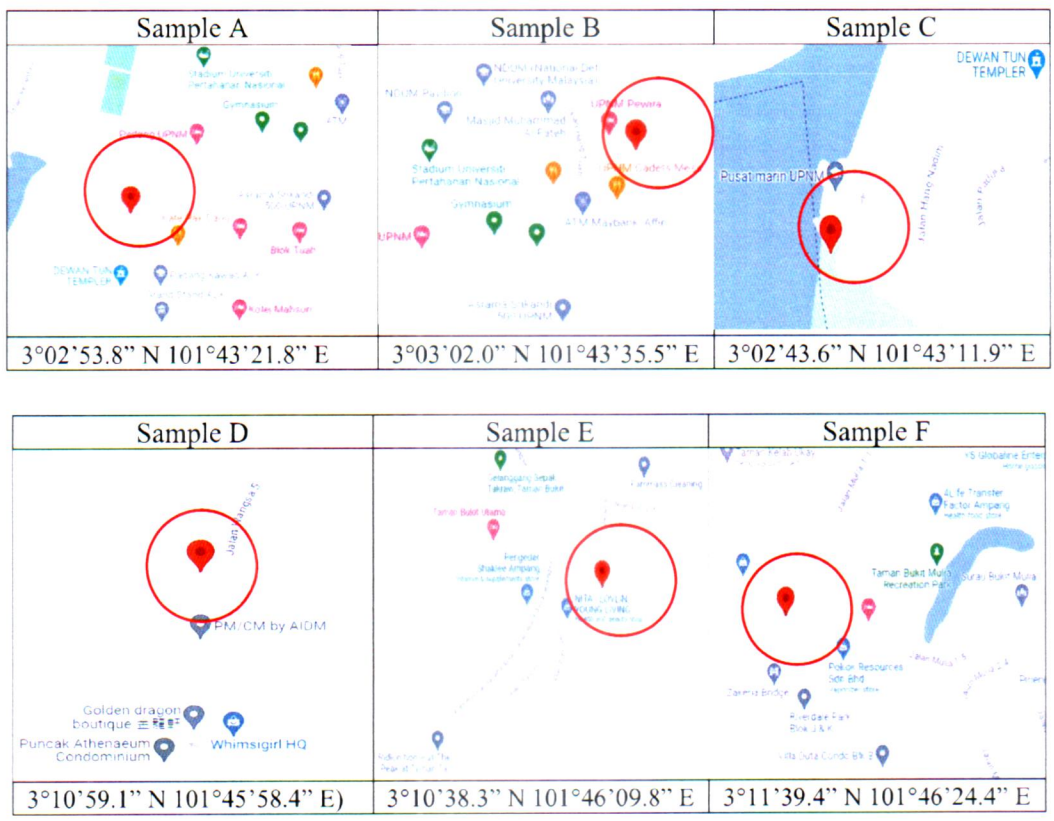

Fig. 1 Sampling locations

Basic soil properties

Basic soil properties were held for soil classification, such as sieve analysis, Atterberg limit, moisture content, and bulk density. Shear strength parameters were evaluated by the box shear box test.

Hydraulic soil properties

Accurate parameters for hydraulic characteristics are essential for modelling soil-water interaction and understanding how soil responds to rainfall. The plate pressure extractor test, which determines the soil water characteristic curve (SWCC), is another crucial factor in simulating rainfall-induced slope stability. The pressure plate testing uses a total of eight weight chambers operating within a pressure range of 0 to 15 bar. We create a graph for each soil sample based on the results, which illustrates the relationship between volumetric water content and pressure (matric suction). The Van Genuchten (1980) model is then used to fit a soil water retention curve to each graph. Ultimately, the graph depicting the squared fitted regression line for each soil sample can be displayed.

Rainfall intensities

The rainfall intensities for this study were chosen based on real-time monitoring for two different durations: 2 hours and 8 hours. These intensities were measured at all places inside the UPNM campus and Bukit Antarabangsa. The rainfall intensity is classified as low (LL-type rainfall) for an eight-hour downpour, while it is classified as high (SH-type rainfall) for a two-hour rainstorm. The rainfall station located at Seri Kembangan (Station ID: 3017107) within the Petaling district offers two-hour and eight-hour rainfall data specifically for the UPNM area.

The rainfall data for the Bukit Antarabangsa area is collected from two different stations. The two-hour data is taken from the station located in Kampung Kemensah in the Gombak district (Station ID: 0232941RF), while the eight-hour data is received from the station in Bukit Antarabangsa (Station ID: 3117080).

The Seri Kembangan rainfall station recorded SH-type rainfall at the UPNM campus on April 18, 2023. The cumulative rainfall of 98 millimetres over a period of two hours results in an average rainfall intensity of 48 mm/hr. On April 7, 2023, the Seri Kembangan rainfall station recorded low-intensity, or LL-type, rainfall. The cumulative rainfall over the course of eight hours is 32.5 millimetres, resulting in an average rainfall intensity of 4.1 millimetres per hour.

On May 7, 2023, in the Kampung Kemensah rainfall station in Bukit Antarabangsa, there were high intensities of SH-type rainfall noted. The Bukit Antarabangsa (Oakleaf) rainfall station recorded a cumulative rainfall of 43 millimetres for a period of two hours on April 8th, 2023. This corresponds to an average rainfall intensity of 21.5 mm/h, indicating LL-type rainfall. The cumulative rainfall over the course of eight hours is 34.5 millimetres, resulting in an average rainfall intensity of 4.3 millimetres per hour. The summary of the SF and LL type for both sites are shown in **Table 1**.

Table 1 Rainfall intensity for SS and LL types.

Rainfall Intensity	UPNM campus (mm/hr)	Bukit Antarabangsa (mm/hr)
2-Hour rainfall (SH- type)	48	21.5
8-Hour rainfall (LL-type)	4.1	4.3

Parameters for numerical simulations

A series of experiments will use the soil samples collected from different. These experiments aim to determine the essential parameters needed for the software simulation, such as soil matric suction, hydraulic conductivity of soil, soil cohesion, and soil internal friction angle. We will accomplish the objective of this research by conducting parametric simulations that meet the necessary soil characteristics for the GeoStudio software to simulate a range of slopes as in **Table 2.**

Table 2 Slope Simulations for The Six Soil Samples

Parameters	Sets of Simulations			
	1	2	3	4
Slope Height, H (m)	Constant	**Change**	Constant	Constant
Slope Angle, α (°)			**Change**	
Rainfall Intensity, I (mm/h)		Constant	Constant	
Rainfall Duration, D (h)				
Groundwater Level, GWL (m below ground)				**Change**

The Public Works Department (PWD) standard specifies the beginning values for all parameter values, except for rainfall intensity, rainfall duration, and groundwater level. According to PWD's Guidelines for Slope Design, untreated fill slopes and embankments must have six-meter-high berms. The slope gradients for the cut areas should be between 1V:1H and 1V:1.5H, while for the fill areas, they should be 1V:2H. The constant values for slope height, slope angle, and groundwater level have been found as six metres, 35 degrees, and seven metres, respectively. To facilitate the completion of the parametric studies, there are three extra proposed values for slope height, slope angle, and groundwater level. Furthermore, each of the four sets of simulations will undergo two and eight hours of rainfall, followed by 22 and 16 hours of monitoring, respectively.

Numerical simulations set

Set 1

Both sets must use constant values of six metres for slope height, 35 degrees for slope angle, and seven metres for groundwater level. In addition, both sets of model slopes will undergo rainfall of two and eight hours, respectively.

Set 2 and II

Simulations Set 2A, 2B, and 2C, and Simulations Set IIA, IIB, and IIC are with constant values for all parameters except for slope height. In these instances, the inclination angle and water table values must remain constant at 35° and seven metres, respectively. However, the height of the slope will vary, with Set 2A and IIA having a height of two metres, set 2B and IIB having a height of four metres, and Set 2C and IIC having a height of eight metres. Simulations Set 2A, 2B, and 2C will subject the model slopes to two hours of rainfall, while Simulations Set IIA, IIB, and IIC will experience eight hours of rainfall. The third set of simulations, known as Simulations Set 3, maintains constant values for all parameters, except for the slope angle.

Set 3 and III

Simulations Set 3A, 3B, and 3C, and Set IIIA, IIIB, and IIIC using slope height and groundwater level which will remain constant at six and seven metres, respectively. However, the slope angle is changed to 25 degrees for Sets 3A and IIIA, 45 degrees for Sets 3B and IIIB, and 55 degrees for Sets 3C and IIIC with two hour and eight-hour rainfall.

Set 4 and IV

Simulation Set 4 involves using constant values for all parameters, except for the groundwater level. In these instances, the measurements for slope height and angle will remain constant at six metres and 35 degrees, respectively. However, the groundwater levels are changed to one meter for Sets 4A and IVA, three meters for Sets 4B and IVB, and five meters for Sets 4C and IVC. Simulations Set 4A, 4B, and 4C will experience a total of two hours of rainfall on the model slopes, while Simulations Set IVA, IVB, and IVC will experience a total of eight hours of rainfall. The summary of all cases is as shown in **Table 3**.

Table 3 Planning of the numerical simulation

Parameters	**Rainfall type**		**Slope Height, H (m)**	**Slope Angle α (°)**	**Rainfall Intensity,I (mm/h)**						**GWL (m)**	**Remarks**
Set	**SH-2hr**	**LL-8hr**			**A**	**B**	**C**	**D**	**E**	**F**		
1a	1		6	35	48			21.5			7	INITIAL
1b		1	6	35	4.1			4.3			7	CASE
2a	1		**2**	35							7	CHANGE
2b	1		**4**	35	4.8			21.5			7	SLOPE
2c	1		**8**	35							7	HEIGHT
IIA		1	**2**	35							7	
IIB		1	**4**	35	4.1			4.3			7	
IIC		1	**8**	35							7	
3a	1		6	**25**							7	CHANGE
3b	1		6	**45**	4.8			21.5			7	SLOPE
3c	1		6	**55**							7	ANGLE
IIIA		1	6	**25**							7	
IIIB		1	6	**45**	4.1			4.3			7	
IIIC		1	6	**55**							7	
4a	1		6	35							**1**	CHANGE
4b	1		6	35	4.8			21.5			**3**	GWL
4c	1		6	35							**5**	
IVA		1	6	35							**1**	
IVB		1	6	35	4.1			4.3			**3**	
IVC		1	6	35							**5**	
											Total simulation	**120**

Geometry of slope for numerical simulations

Real-time rainfall intensities and durations, different groundwater levels, and various slope angles and heights will all be applied to the series of model slopes that have been created in the simulations. The study will be conducted in two main stages, with the investigation of slope stability coming after the analysis of groundwater seepage and excess pore-water development. In the GeoStudio SEEP/W module, seepage analyses can only be carried out using

the finite element approach, whereas the SLOPE/W module's slope stability analyses may be performed using the Morgenstern-Price limit equilibrium method. The outcomes of slope stability analyses are presented in terms of slope safety factors. The slope model's top and bottom sides shall be three times longer than its height during simulation (Satyanaga 2022). Given that raindrops may seep into surrounding soil on both sides, it is a suitable value for minimising the influence of boundary conditions from the left and right sides of the model (Satyanaga 2022). The slope simulation models shall therefore be drawn according to **Fig. 2.**

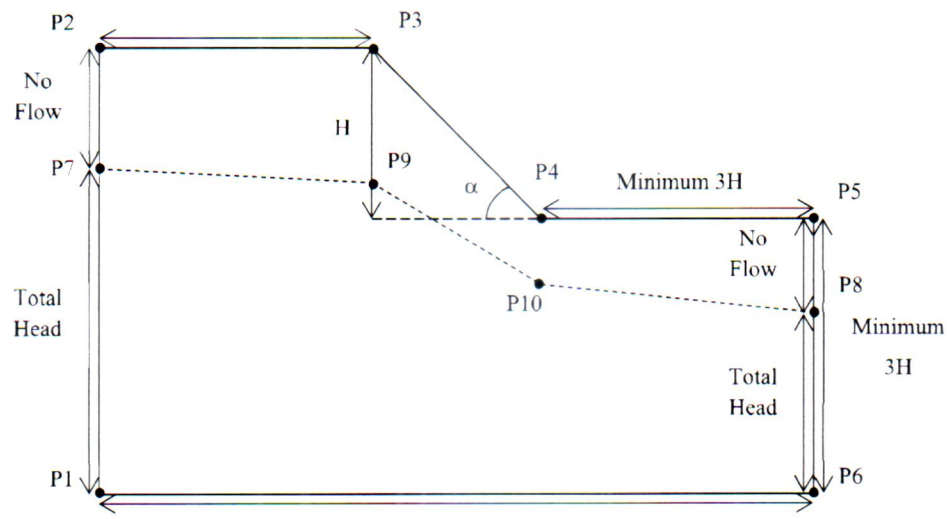

Fig. 2 Geometry of The Model Domain Geostudio

Results and Discussions

Sieve analysis

The examination of different soil samples demonstrates clear differentiation in their gradation properties. Soil sample A is categorised as well-graded sand with gravel (SW) and has a coefficient of uniformity (C_u) of 10.682 and a coefficient of curvature (C_c) of 1.172. Soil sample D is classified as well-graded sand with gravel (SW), and it has C_u and C_c values of 10.796 and 1.130, respectively. Furthermore, soil sample E, which is also classified as well-graded sand with gravel (SW), exhibits higher gradation values, with a coefficient of uniformity (C_u) of 13.715 and a coefficient of curvature (C_c) of 1.374. The classification of soil sample B as poorly graded sand with gravel (SP) yields a Cc value of 0.996, while soil sample C, also classified as SP, displays a C_c value of 0.728. Finally, we classify soil sample F as poorly graded sand with gravel (SP), based on a coefficient of curvature (C_c) of 0.970. The gradation metrics highlight the differences in soil texture and classification among the samples. Particle size distribution curve for all samples is shown in **Fig. 3 (a)** and **(b),** while **Table 4** is the summary of soil samples' properties.

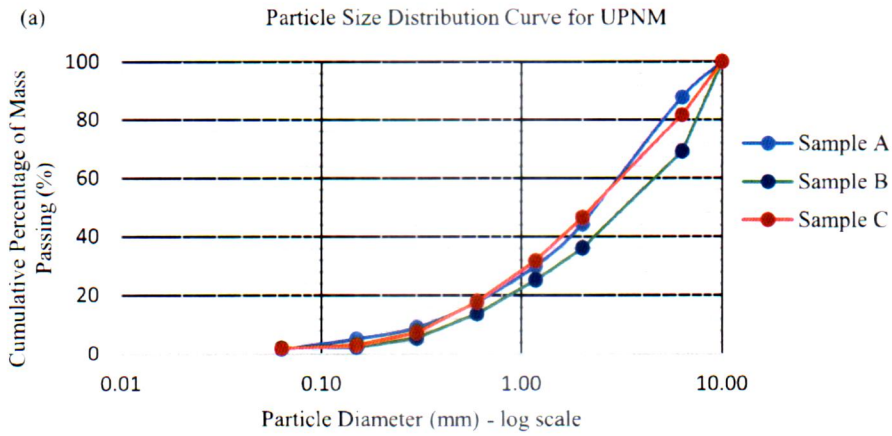

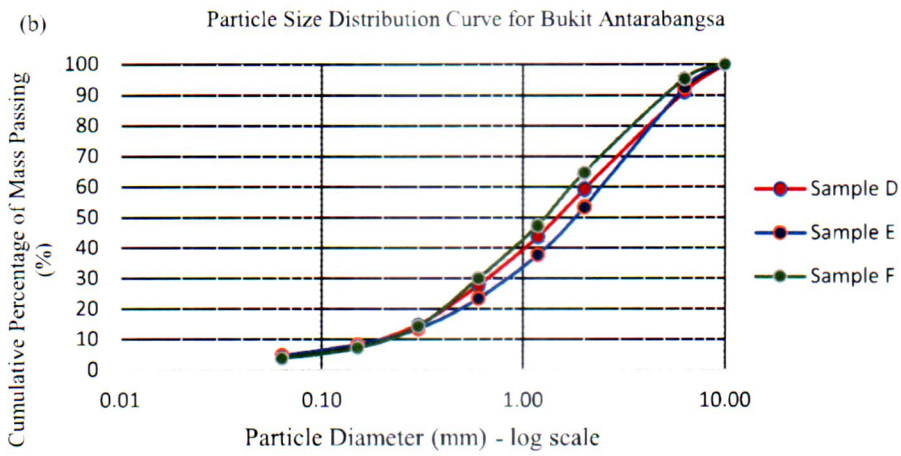

Fig. 3 (a) and (b) Soil Sample of UPNM and Bukit Antarabangsa Particle Size Distribution Curve

Table 4 Soil samples parameters

Parameters	Soil Samples					
	A	**B**	**C**	**D**	**E**	**F**
PSD						
C_U	10.68	10.96	9.716	10.80	13.72	8.48
C_C	1.72	0.996	0.893	1.130	1.374	0.970
Soil classification	SW Well-graded sand with gravel	SP Poorly graded sand with gravel	SP Poorly graded sand with gravel	SW Well-graded sand with gravel	SW Well-graded sand with gravel	SP Poorly graded sand with gravel
Hydraulic conductivity, *k (m/s)*	2.08E-05	1.21E-05	8.57E-06	3.64E-06	6.32E-06	5.83E-06
Cohesion, *c' (kPa)*	20	0.075	3.4	7.6	6.0	13.6
Internal Friction Angle, Φ (°)	45	40	41	33	46	39
Unit Weight, γ *(kN/m³)*	14	13	15	16	16	16
Residual Volumetric Water Content, θ_r	1.000E-10	0.349	0.183	1.00E-10	0.254	0.484
Saturated Volumetric Water Content, θ_s	0.428	0.471	0.507	0.494	0.644	0.581

Soil-Water Characteristic Curve (SWCC)

The graph shows in **Fig. 4** for the Soil-Water Characteristic Curves (SWCCs) are for six different soil samples (A, B, C, D, E, and F). The graph reveals that Soil Sample A, classified as well-graded sand with gravel (SW), begins with a volumetric water content of approximately 0.45 and steadily decreases, maintaining a relatively high-water content compared to other samples. The soil sample B, classified as poorly graded sand with gravel (SP), starts with a high initial water content above 0.5, which gradually decreases with increasing matric suction. Soil Sample C (SP) has a relatively stable water content between 0.45 and 0.4, with minimal changes over the matric suction range. Soil sample D (SW) exhibits a gradual decrease in volumetric water content from about 0.35 to 0.3, indicating moderate retention capacity. Notably, soil sample E (SW) starts with the highest initial water content (near 0.6) and maintains the highest water retention across the matric suction range. Conversely, soil sample F (SP) starts with a higher initial water content, around 0.45, but shows a significant drop, ending below 0.2 at the highest matric suction.

After analysing these results, well-graded sands with gravel (SW), such as samples A, D, and E, generally exhibit superior water retention characteristics, with sample E retaining the most water at all levels of matric suction. On the other hand, poorly graded sands with gravel (SP), represented by samples B, C, and F, display lower initial water content and more significant decreases in water content with increasing matric suction. Comparative analysis shows that soils with higher coefficients of uniformity (Cu) and curvature (Cc), such as samples A, D, and E, are better at holding water. On the other hand, sands that are not graded well (samples B, C, and F) are worse at holding water, which shows that they lose this ability as matric suction increases. This graph effectively elucidates the variations in water retention characteristics among the six soil samples, underscoring the impact of soil gradation on their hydrological properties.

Upon analysis of the hydraulic conductivity as shown in **Fig. 5**, it is clear that well-graded sands with gravel (SW), namely samples A, D, and E, exhibit different degrees of reduction in water conductivity as matric suction increases. Sample D displays a significant decrease. The poorly graded sands with gravel (SP), which are represented by samples B, C, and F, often have greater beginning conductivities. However, samples C and F show a more progressive decrease over time. This graph clearly demonstrates the variations in water conductivity across the six soil samples, highlighting the impact of soil gradation and suction levels on the hydraulic properties of the soil.

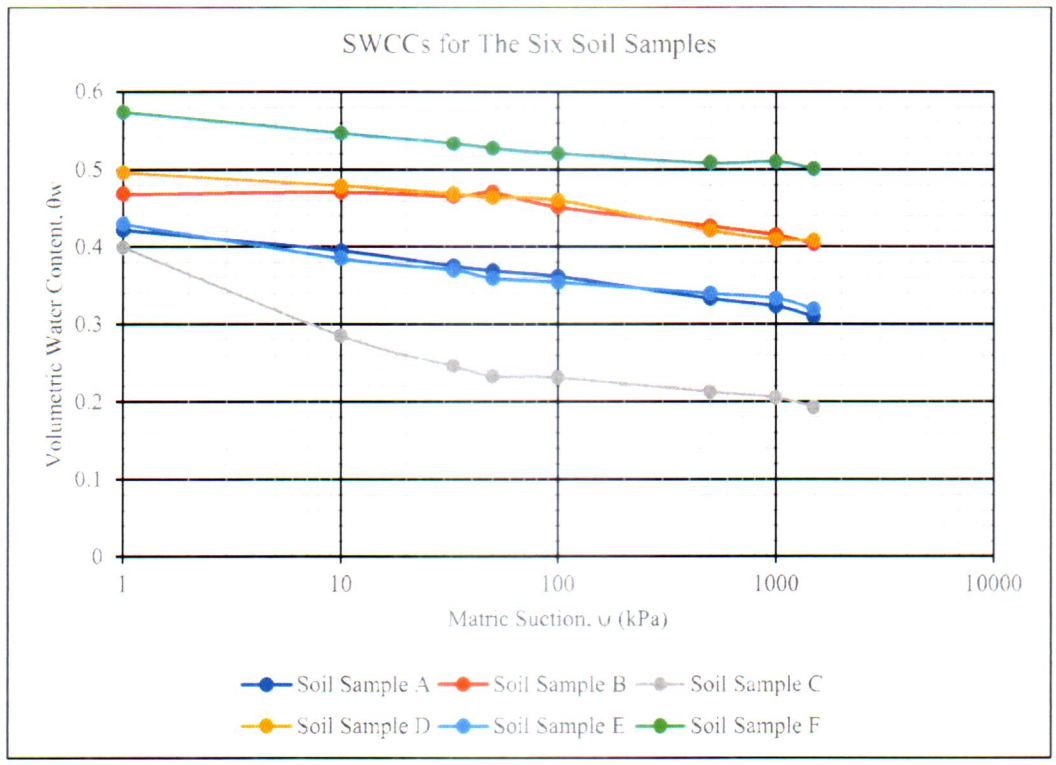

342
343
344
345

Fig. 4 SWCC Comparison for The Six Soil Samples

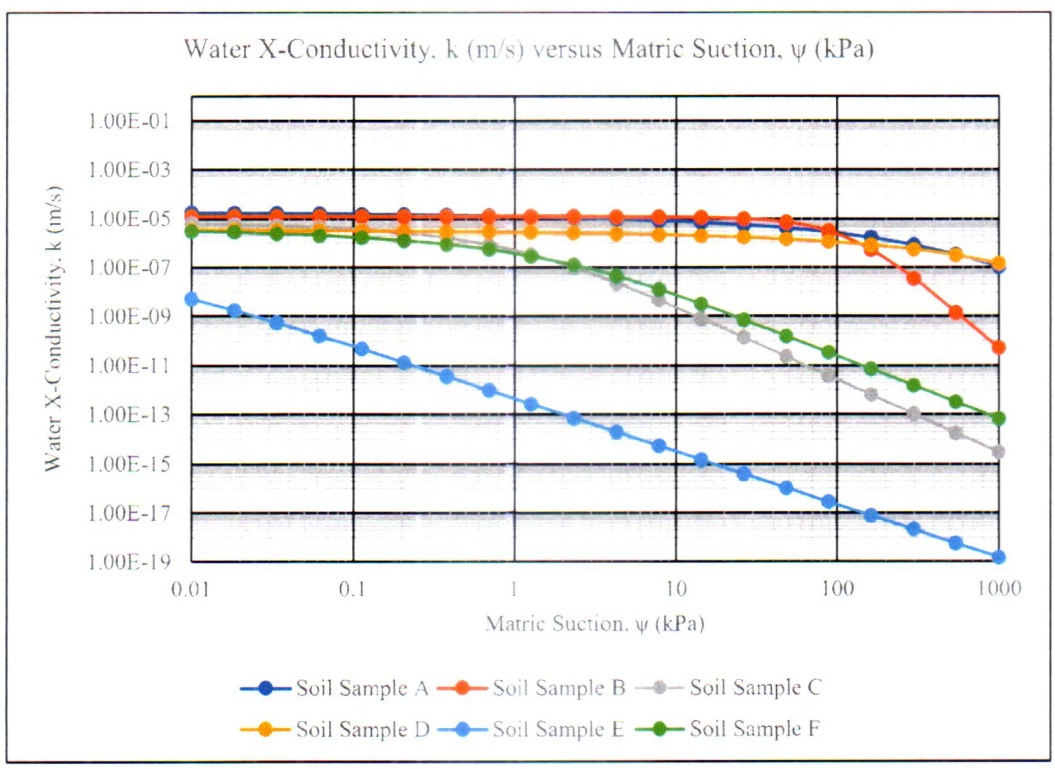

346
347
348
349

Fig. 5 Hydraulic conductivity comparison for The Six Soil Samples

350

351

Factor of Safety

The results of GeoStudio's slope stability analyses indicate that variations in slope height and angle have an impact on the safety factors of six different slopes. However, the safety factors for slopes exposed to a two-hour rainfall and slopes exposed to an eight-hour rainfall remain constant, as shown in **Table 5**. However, the analysis reveals that the safety factors for slopes experiencing a two-hour rainfall differ from those for slopes exposed to an eight-hour downpour when the groundwater level lowers from seven metres to one metre.

Based on the findings, the same assumption applies to slopes exposed to rainfall during two and eight hours when the groundwater level is raised to three metres. The initial condition occurs when the safety factors for slopes exposed to two- and eight-hour rainfall remain the same, despite the groundwater level increasing to five meters. **Table 5** indicates that slopes exposed to an eight-hour rainstorm maintain consistent safety parameters at groundwater depths over one meter.

Different soil samples may belong to the same soil classification, but the residual volumetric water content (VWC) and saturated VWC values were different in each sample, as shown by the pressure plate tests. Soil samples A, D, and E are classified as SW soils. Soil Samples A and D have a residual volumetric water content (VWC) value of 1E-10; however, Soil Sample E has a significantly higher residual VWC value of 0.2549. Currently, these three soil samples exhibit distinct saturated volumetric water content (VWC) values, particularly measuring 0.4281, 0.4942, and 0.6449, respectively. On the other hand, we classify soil samples B, C, and F as SP soils. The residual volumetric water content (VWC) values in the three soil samples are 0.3498, 0.1835, and 0.4843, respectively. The saturated VWC values for the same samples are 0.4710, 0.5072, and 0.5816, respectively. The slope's safety factor varies depending on the residual volumetric water content (VWC) and saturated VWC values for each soil sample, even if they have the same soil classification.

Slope Stability Relationships with Slope Geometry, Groundwater Level and Rainfall

Each soil sample delivers a varied safety factor under a series of variations in slope geometry, groundwater level, and rainfall intensity and duration due to the combined effects of the soil matric suction, hydraulic conductivity, effective internal friction angle, and effective cohesion. In contrast to the other five soil samples, Soil Sample A has the greatest safety factor range, as shown in **Fig. 6**, while Soil Sample B has the lowest range. This can be because Soil Sample A has the highest cohesion value whereas Soil Sample B has the lowest cohesion value. Higher soil cohesion results in more stable slopes as it provides the soil with the internal strength that it requires to resist shear forces. Meanwhile, the second and third highest safety factor ranges, fall under Soil Samples F and E, respectively. Whereas the safety factor ranges for Soil Samples C and D are comparable.

The results demonstrate that only slopes with Soil Sample B have safety factors that are less than one; these values are 0.889 and 0.635 for slopes that are six metres high, have a groundwater depth of seven metres, and are inclined at 45 and 55 degrees, respectively. When the slopes are six metres high, sloped at 35°, have one metre of groundwater depth, and are subjected to two and eight hours of rainfall, respectively, the safety factors of slopes comprised of Soil Sample B are also less than one and are 0.593 and 0.988, respectively.

Even though a slope's safety is implied by a safety factor of one, several agencies, including PWD, advocate using a safety factor of 1.5 as the standard minimum value to use in calculations. According to this guideline, the

35 degrees slopes formed by Soil Sample B are deemed risky once they reach a height of two metres or more since the minimal safety factor at that height is just 1.301. Furthermore, the six metres high slopes with Soil Sample C are possibly hazardous when the slopes are 45 and 55 degrees since the safety factors obtained are only 1.454 and 1.196, respectively. In addition, when the six metres high slope is inclined at 55°, the safety factor for the slope with Soil Sample D is 1.266, which is also below the acceptable limit. When the slopes have three metres or more of groundwater depth and are subjected to two and eight hours of rainfall, the safety factors of slopes with six metres of height, sloped at 35°, and comprised of Soil Sample B remain unsatisfactory. When the six-metre-high and 35° slopes are subjected to a two-hour rainfall and the groundwater level is one metre, slopes with Soil Samples C and D are also considered potentially dangerous since the safety factors are only 1.476 and 1.338, respectively.

In summary, the slopes formed by Soil Sample B are unsafe when they are two metres high or above, inclined at 35° or higher, and have a groundwater depth of one to seven metres during the two- and eight-hour rainfall events. For slopes with Soil Sample C, the six-meter-high slopes are potentially hazardous when they are slanted at 45° or higher, but for slope with Soil Sample D, the slope is dangerous when it is sloped at 55°. When the groundwater level is one metre deep and there is a two-hour rainfall, the slopes with Soil Samples C and D are also possibly dangerous.

The safety factor for each soil sample decreases as the slope height increases, as can be observed in Figure 6. According to the analyses of Pearson's correlation coefficient, the slope height and safety factor have a highly significant opposing linear relationship for each of the soil samples. The correlation coefficients, r, for Soil Samples A, B, C, D, E, and F are -0.93950, -0.92499, -0.94395, -0.93734, -0.94932, and -0.93846, respectively. In comparison to the other soil samples, Soil Sample B has the lowest correlation coefficient, while Soil Sample E exhibits the strongest correlation between the slope height and safety factor. On the other hand, Soil Samples A, D, and F have almost similar correlation coefficients, resulting in displayed lines for these three soil samples that are nearly parallel to one another on the plotted graph.

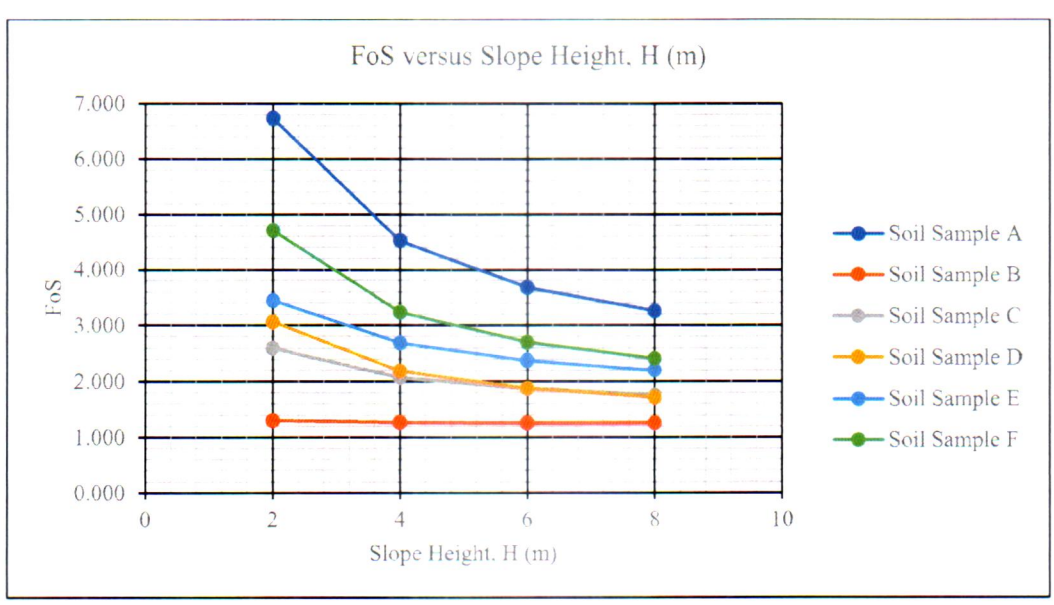

Fig. 6 Safety Factors of Soil Samples versus Slope Height, H (m)

421

422 **Table 5.** Result of FoS for all cases

423

Parameters	Soil sample name	SET NAME																		
		1a	1b	2a	2b	2c	IIA	IIB	IIC	3a	3b	3c	IIIA	IIIB	IIIC	4a	4b	4c	IVA	IVB	IVC
Case name		INITIAL CASE		CHANGE OF SLOPE HEIGHT						CHANGE OF SLOPE ANGLE						CHANGE OF GWL					
Rainfall type SH-2hr		P		P	P	P				P	P	P				P	P	P			
Rainfall type LL-8hr			P				P	P	P				P	P	P				P	P	P
Slope Height,H (m)		6	6	2	4	8	2	4	8	6	6	6	6	6	6	6	6	6	6	6	6
Slope Angle a (°)		35	35	35	35	35	35	35	35	25	45	55	25	45	55	35	35	35	35	35	35
GWL (- m)		7	7	7	7	7	7	7	7	7	7	7	7	7	7	1	3	5	1	3	5
Rainfall Intensity, I (mm/h)	A	4.8	4.1	4.8			4.1			4.8			4.1			4.8			4.1		
	B																				
	C																				
	D	21.5	4.3	21.5			4.3			21.5			4.3			21.5			4.3		
	E																				
	F																				
Factor of Safety (FoS)	A	3.7	3.7	6.7	4.5	3.3	6.7	4.5	3.3	4.6	3.1	2.6	4.6	3.1	2.6	2.9	3.4	3.7	3.1	3.7	3.7
	B	1.3	1.3	1.3	1.3	1.3	1.3	1.3	1.3	1.8	0.9	0.6	1.8	0.9	0.6	0.6	1.1	1.3	1.0	1.3	1.3
	C	1.9	1.9	2.6	2.1	1.8	2.6	2.1	1.8	2.6	1.5	1.2	2.6	1.5	1.2	1.5	1.9	1.9	1.6	1.9	1.9
	D	1.9	1.9	3.1	2.2	1.7	3.1	2.2	1.7	2.5	1.5	1.3	2.5	1.5	1.3	1.3	1.7	1.9	1.5	1.9	1.9
	E	2.4	2.4	3.4	2.7	2.2	3.4	2.7	2.2	3.2	1.9	1.5	3.2	1.9	1.5	2.2	2.4	2.4	2.2	2.4	2.4
	F	2.7	2.7	4.7	3.2	2.4	4.7	3.2	2.4	3.4	2.2	1.9	3.4	2.2	1.9	2.2	2.7	2.7	2.2	2.7	2.7
**Remarks:		Base failure			1		FoS<1.3														

424

As demonstrated in **Fig. 7**, the safety factor for each soil sample decreases as the slope angle increases. The correlation coefficient analyses suggest an extremely substantial negative linear relationship between the safety factor and slope angle for each of the soil samples. For Soil Samples A, B, C, D, E, and F, the correlation coefficients are -0.98591, -0.98234, -0.97780, -0.98289, -0.98227, and -0.98483, respectively. Soil Sample A exhibits the most significant negative relationship between the slope height and safety factor, whereas Soil Sample C has the lowest correlation coefficient when compared to the other soil samples. The displayed lines for Soil Samples B, D, and E on the plotted graph are almost parallel to one another as these three soil samples have approximately similar correlation coefficients. By comparing the overall correlation coefficients for all of the soil samples in **Fig. 7** and **Fig. 8**, it can be observed that lowering slope height increases the safety factor at a higher rate than decreasing slope angle.

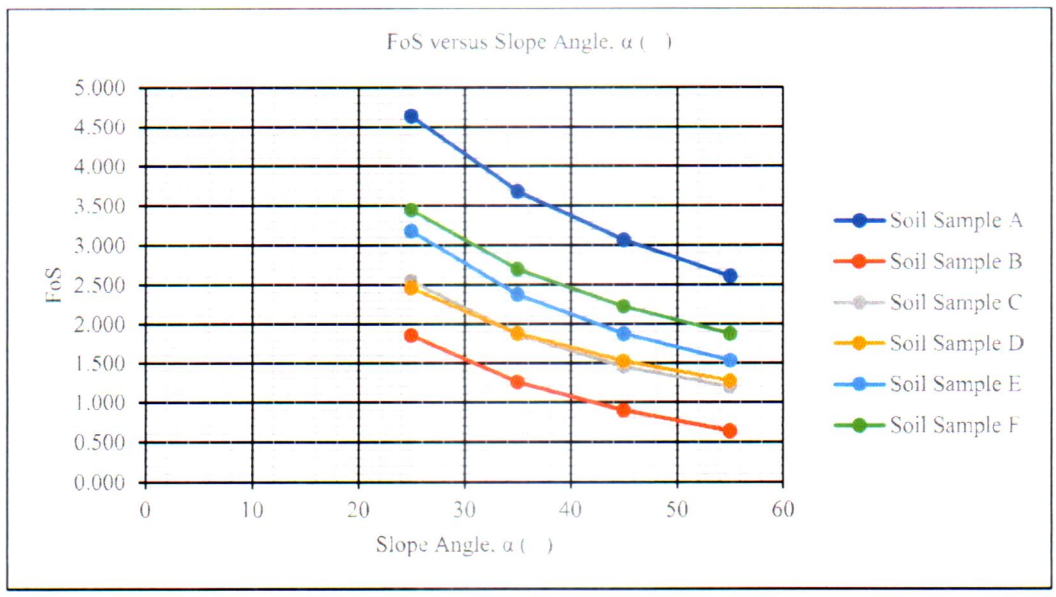

Fig. 7 Safety Factors of Soil Samples versus Slope Angle, ( )

As seen in **Fig. 8**, the safety factor for each soil sample increases as the groundwater level increases until it reaches a constant value at a groundwater level of five metres. The groundwater level and safety factor have a strong positive linear relationship for each soil sample, according to correlation coefficient analyses. For Soil Samples A, B, and D, the correlation coefficients are 0.922, 0.900, and 0.909, respectively. While the correlation coefficient for Soil Samples C, E, and F is 0.7746, respectively, therefore the displayed lines for these three soil samples are almost parallel to one another on the plotted graph. The strongest positive relation between the groundwater level and safety factor can be observed in Soil Sample A, whereas Soil Samples C, E, and F have the lowest correlation coefficients.

The safety factor for each soil sample increases as the groundwater level rises, as shown in **Fig. 9,** until it reaches a constant value at three metres. Analyses of the correlation coefficient indicate the groundwater level and safety factor have a significant positive linear correlation for each soil sample. The correlation coefficient across all soil samples is 0.774. Since all of the soil samples have the same correlation coefficients, their displayed lines on the plotted graph are almost parallel to one another.

454 It is clear from comparing the overall correlation coefficients in **Fig. 8** and **Fig. 9** that the safety factor develops
455 higher during an eight-hour downpour than during a two-hour rainfall. This can be a result of the eight-hour
456 rainfall's low intensity, which gives the moisture in the soil enough time to evaporate during the monitoring hour,
457 lowering the soil moisture content, increasing matric suction, restoring the soil shear strength, and thus improving
458 slope stability. Also, considering the low rainfall intensity has minimal effect on the three metres and above
459 groundwater depths, the safety factor for slopes subjected to eight hours of rainfall achieves constant values at a
460 shallower groundwater depth than the safety factor of slopes subjected to two hours of rainfall.
461

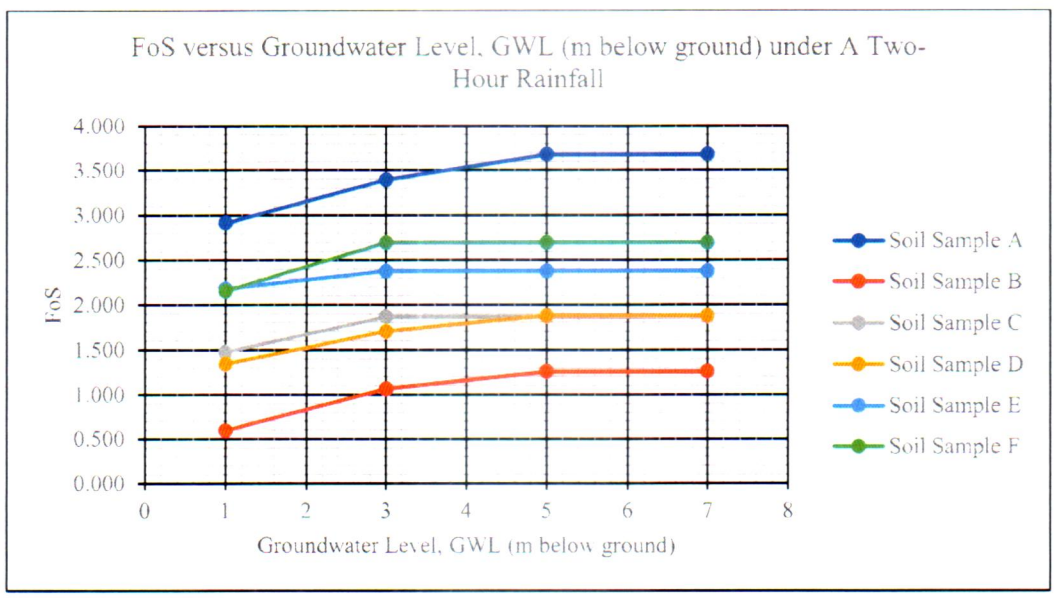

462
463 **Fig. 8** Safety Factors of Soil Samples versus Groundwater Level, GWL (m below ground) under A Two-Hour
464 Rainfall
465
466 When it rains, the slope's moisture content increases, causing a drop in the soil's matric suction or negative
467 pore-water pressure, as well as its effective stress and shear strength. This ultimately leads to the slope's failure.
468 When comparing the slopes that experienced two hours of rainfall with those that experienced eight hours of
469 rainfall, the negative pore-water pressure range at the upper sides of the slopes subjected to eight hours of rainfall
470 is greater than or similar to the negative pore-water pressure range for the slopes subjected to two hours of rainfall.
471 The low intensity of the eight-hour rainfall, which allowed sufficient time for evaporation and prevented further
472 infiltration into the groundwater table, could be the reason for this. Consequently, the moisture content on slopes
473 dropped. Furthermore, for slopes with groundwater depths of seven, five, and three meters, the rise in groundwater
474 level during rainfall is negligible. Thus, a decrease in matric suction initiates the slope instability without a
475 corresponding increase in pore-water pressure to a positive level. Exceptions are provided for slopes that have a
476 groundwater depth of one metre in Simulations Set 4A and IVA, as well as slopes that have soil samples A, B, and
477 D in Simulations Set 4B. During rains, the groundwater level on these slopes rises significantly. The decrease in
478 matric suction led to slope instability, resulting in a positive pore-water pressure and an increase in the groundwater
479 level.
480 Overall, each soil sample demonstrates exhibits distinctive characteristics in terms of matric suction,
481 hydraulic conductivity, effective internal friction angle, and effective cohesion. While the slope conditions may

be the same for all soil samples in simulations, the distinct combination of hydraulic and mechanical characteristics results in each sample having a different slope safety factor. Furthermore, the analytical results indicated that the safety factor of a slope decreases with an increase in both slope height and angle. Conversely, the safety factor of a slope rises in proportion to the groundwater level. Moreover, the analyses demonstrate that the matric suction decreases as the soil moisture content increases. When comparing the slopes that experienced two and eight hours of rainfall, there is still a significant variation in the negative pore-water pressure within each slope slip surface. The safety factors of the slopes exposed to two and eight hours of rainfall remain unchanged. This is because the minimal change in rainfall intensity remains sufficient to create a difference in safety factors.

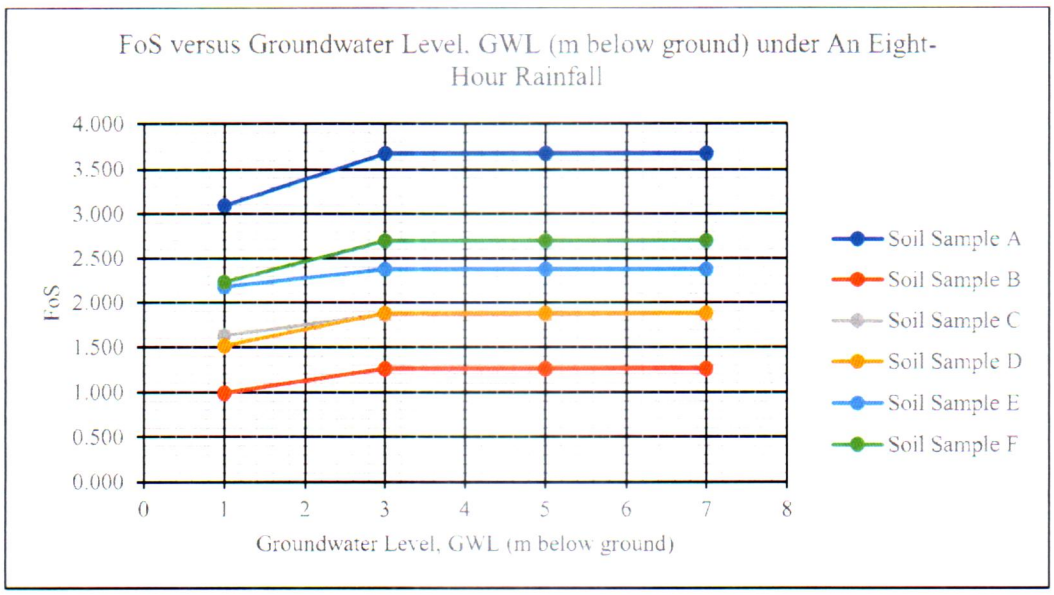

Fig. 9 Safety Factors of Soil Samples versus Groundwater Level, GWL (m below ground) under An Eight-Hour Rainfall

Conclusions

The effect of soil suction for various types of unsaturated soils under normal to critical rainfall conditions, as well as the corresponding safety factors, can be accurately determined through comprehensive analysis. Findings from slope stability analyses reveal an interaction between soil suction and moisture content induced by rainfall. The increase in soil moisture content, resulting from decreased soil suction, reduces soil shear strength, eventually leading to slope failure. Each soil sample exhibits unique values for matric suction, hydraulic conductivity, effective internal friction angle, and effective cohesion. Consequently, these varying hydraulic and mechanical properties contribute to distinct slope safety factors for each soil sample, even under identical slope conditions during simulations. The unique soil suction characteristics of the six soil samples significantly influence the outcomes of slope stability analyses, enabling precise assessment of slope hazards during rainfall events lasting two and eight hours.

Further research is necessary to investigate the variations in slope safety factors under different rainfall intensities, particularly heavy rainfall. Future studies should consider actual slope geometry and groundwater

conditions identified in the field where soil samples are collected. Additionally, similar analyses should be conducted on a broader range of soil types, especially on non-homogeneous slopes comprising multiple soil types.

Considering the hysteresis exhibited by the Soil-Water Characteristic Curve (SWCC) of soil, it is recommended that future research incorporates both wetting and drying SWCCs. In numerical simulations, it is advisable to utilise the wetting soil-water characteristic curve (SWCC) to describe the process of infiltration during wetting. Similarly, the drying SWCC should be employed to simulate evaporation and drainage during the drying phase. This approach accurately represents the moisture dynamics experienced by the soils.

Declarations

Ethics approval and consent to participate Not applicable.
Consent for publication Not applicable.
Competing interests The author declares no competing interests.

Funding
The authors declare that no funds, grants, or other support were received during the preparation of this manuscript. However, the authors appreciate the support from faculty of engineering, Universiti Pertahanan Nasional Malaysia for the laboratory equipment and software provided for this research.

Conflict of interest
The authors have no relevant financial or non-financial interests to disclose.

Acknowledgments
The writers also gratefully acknowledge the support of Universiti Pertahanan Nasional Malaysia.

Credit author statement.
Aniza Ibrahim: Conceptualization, Methodology, Software Tan Yi Xuan: Data curation, Writing- Original draft preparation. Fakhrurazi Awang Kechik: Visualization, Investigation. Aizat Mohd Taib: Software, Validation.: Dayang Zulaika Abang Hasbollah and Mohd. Firdaus Md Dan@Azlan: Writing- Reviewing and Editing,

References

Abeykoon T, Gallage C, Dareeju B, Trofimovs J (2018) Real-time monitoring and wireless data transmission to predict rain-induced landslides in critical slopes. Australian Geomechanics Journal 53(3):61–76

Abeykoon T, Gallage C, Trofimovs J (2019) Optimisation of sensor locations for reliable and economical early warning of rainfall-induced landslides In Proceedings of the Ninth International Conference on Geotechnique, Construction Materials, and Environment (GEOMATE 2019), Japan (pp 69–74) GEOMATE International Society

Al-Karni A A (2011) Evaluation of shear strength of cohesionless soil due to excess pore water pressure. Arabian Journal of Geosciences 4(7–8):1095–1101

Alsubal S, Sapari N, Bin Harahap I S H Ali Mohammed Al-Bared M (2019) A review on mechanism of rainwater in triggering landslide. IOP Conference Series: Materials Science and Engineering 513(1) https://doi.org/10.1088/1757-899X/513/1/012009

Batterson M, Liverman D G E, Ryan J, Taylor D (1999) The assessment of geological hazards and disasters in Newfoundland: An update Newfoundland. Report No 99–1 Department of Mines and Energy Geological Survey

Baum R L, Godt J W (2010) Early warning of rainfall-induced shallow landslides and debris flows in the USA. Landslides 7(3):259–272

Cerri R I, Reis F A G V, Gramani M F, Giordano L C, Zaine J E (2017) Landslides zonation hazard: Relation between geological structures and landslides occurrence in hilly tropical regions of Brazil Annals of the Brazilian Academy of Sciences 89(4):2609-2623 https://doi.org/10.1590/0001-3765201720170224

Chen H, Lee C F, Law K T (2004) Causative mechanisms of rainfall-induced fill slope failures. Journal of Geotechnical and Geoenvironmental Engineering 130(6):593–602

Collins B D, Znidarcic D (2004) Stability analyses of rainfall induced landslides. Journal of Geotechnical and Geoenvironmental Engineering 130(4):362–372

562 Cruden D M (1991) A simple definition of a landslide. Bulletin of the International Association of Engineering Geology
563 43:27–29

564 Di BF, Stamatopoulos CA, Stamatopoulos AC, Liu EN, Balla L (2021) Proposal, application and partial validation of a
565 simplified expression evaluating the stability of sandy slopes under rainfall conditions. Geomorphology 395:107966

566 Gallage C, Abeykoon T, Uchimura T (2021) Instrumented model slopes to investigate the effects of slope inclination on
567 rainfall-induced landslides. Soils and Foundations 61(1):160–174 https://doi.org/10.1016/j.sandf.2020.11.006

568 Han B, Hou S S, Zhu B ,Wang L C, Li A ,Ye H J (2014) Deformation monitoring and prediction of a reservoir landslide in
569 Sichuan Province, China .Applied Mechanics and Materials 2694-2701

570 Hou X, Li T, Qi S, Guo S, Li P, Xi Y, Xing X (2021) Investigation of the cumulative influence of infiltration on the slope
571 stability with a thick unsaturated zone. Bulletin of the International Association of Engineering Geology 80:5467–5480

572 Huang G, Zheng M, Peng J (2021) Effect of Vegetation Roots on the Threshold of Slope Instability Induced by Rainfall and
573 Runoff. Geofluids 2021:6682113

574 Huat B B K, Ali F, Hj (2012) Slope hazard assessment in urbanized area. Electronic Journal of Geotechnical Engineering
575 17:341–352 Available at: https://www.researchgate.net/publication/267779830

576 Ibrahim A, Ahmad I K, Taha M R (2018) 3D real-time images of rainfall infiltration into unsaturated soil slope. International
577 Journal of GEOMATE 14(43):31-35 https://doi.org/10.21660/2018.43.3528

578 Ibrahim A, Mukhlisin M, Jaafar O (2013) Numerical assessment of rainfall infiltration into soil column for the unsaturated
579 layered residual forest soil .Jurnal Teknologi 65(2) https://doi.org/10.11113/jt.v65.2200

580 Jamaludin S, Bujang B K H, Omar H (2012) Evaluation and development of cut–slope assessment systems for Peninsular
581 Malaysia in predicting landslides in granitic formation. Jurnal Teknologi 44(1):31-46

582 Kazmi D, Qasim S, Harahap I S H, Baharom S, Imran M, Moin S (2016) A study on the contributing factors of major landslides
583 in Malaysia. Civil Engineering Journal 2(12):669–678

584 Kechik F A, Ibrahim A, Abu Hassan Z, Matlan S J, Taib A M, Rahman N A (2023) Analysis of influence of air-entry values
585 to unsaturated soil properties. Physics and Chemistry of the Earth Parts A/B/C 129:103340
586 https://doi.org/10.1016/j.pce.2022.103340

587 Kristo C, Rahardjo H, Satyanaga A (2019) Effect of hysteresis on the stability of residual soil slope. International Soil and
588 Water Conservation Research 7(3):226–238 https://doi.org/10.1016/j.iswcr.2019.05.003

589 Kristo C, Rahardjo H, Satyanaga A (2019) Effect of hysteresis on the stability of residual soil slope. International Soil and
590 Water Conservation Research

591 Lee L M, Gofar N, Rahardjo H (2009) A simple model for preliminary evaluation of rainfall-induced slope instability.
592 Engineering Geology 108(3):272–285

593 Li Q, Huang D, Pei S, Qiao J, Wang M (2021) Using Physical Model Experiments for Hazards Assessment of Rainfall-Induced
594 Debris Landslides. Journal of Earth Science 32:1113–1128

595 Liu Y, Deng Z, Wang X (2021) The Effects of Rainfall, Soil Type and Slope on the Processes and Mechanisms of Rainfall-
596 Induced Shallow Landslides. Applied Sciences 11(24):11652 https://doi.org/10.3390/app112411652

597 Low T H, Ali F, Ibrahim A S (2012) An investigation on one of the rainfall-induced landslides in Malaysia. Electronic Journal
598 of Geotechnical Engineering 17:435-449

599 Marrapu B M, Kukunuri A, Jakka R S (2021) Improvement in Prediction of Slope Stability & Relative Importance Factors
600 Using ANN. Geotechnical and Geological Engineering 39:5879–5894 https://doi.org/10.1007/s10706-021-01872-2

601 Maturidi A M A M, Kasim N, Taib K A, Azahar W N A W, Tajuddin H B A (2021) Empirically based rainfall threshold for
602 landslides occurrence in Peninsular Malaysia. KSCE Journal of Civil Engineering 25(12):4552–4566
603 https://doi.org/10.1007/s12205-021-1586-4

604 Mousazadeh S, Shariati S, Yousefi M et al (2021) Hexavalent chromium removal using ionic liquid coated magnetic nano
605 zero-valent iron biosynthesized by Camellia sinensis extract. International Journal of Environmental Research 15:1017–
606 1036

607 van Genuchten M T (1980) A closed-form equation for predicting the hydraulic conductivity of unsaturated soils. Soil Sci Soc
608 Am J 44(5):892–898

Pajalić S Peranić J Maksimović S Čeh N Jagodnik V Željko A (2021) Monitoring and Data Analysis in Small-Scale Landslide Physical Model Applied Sciences 11:5040

Petley D (2012) Global patterns of loss of life from landslides. Geology 40(10):927–930

Pour A B, Hashim M (2015) Structural mapping using PALSAR data in the central gold belt, Peninsular Malaysia.Ore Geology Reviews 64(1):13-22 https://doi.org/10.1016/j.oregeorev.2014.06.011

Qasim S, Harahap I S H, Syed Osman S B (2013) Causal factors of Malaysian landslides: A narrative study. Journal of Applied Science and Engineering Technology 5(7):2303–2308

Rahman H A, Mapjabil J (2017) Landslides disaster in Malaysia: An overview. Health and the Environment Journal 8(1):58–71 Available at: https://www.researchgate.net/publication/321096764

Ray A, Bharati A K, Rai R, Singh T N (2021) Landslide occurrences in Himalayan residual soil: A review. Himalayan Geology 42:189–204

Razali I H, Taib M A, Rahman N A, Hasbollah D Z A, Dan M F M, Ramli A B, Ibrahim A (2023) Slope stability analysis of riverbank in Malaysia with the effects of vegetation. Phys Chem Earth Parts A/B/C 129:103334. https://doi.org/10.1016/j.pce.2022.103334

Satyanaga A ,Bairakhmetov N, Kim J R, Moon S-W (2022) Role of bimodal water retention curve on the unsaturated shear strength. Applied Sciences 12:1266 https://doi.org/10.3390/app12031266

Suhaila J, Deni S M, Zawiah W Z, Jemain A A (2010) Trends in Peninsular Malaysia rainfall data during the southwest monsoon and northeast monsoon seasons: 1975–2004. Sains Malaysiana 39(4):533–542

Tariq M, Ali F H, Low T H (2020) An investigation on failure mechanisms and stabilization of landslides in tropical residual soil slopes of Malaysia. Arabian Journal of Geosciences 13:1046 https://doi.org/10.1007/s12517-020-06232-4

Tariq M, Ali F H, Low T H (2020) An investigation on failure mechanisms and stabilization of landslides in tropical residual soil slopes of Malaysia. Arabian Journal of Geosciences 13:1046

Thiebes B (2012) Landslide analysis and early warning systems Springer-Verlag Berlin Heidelberg

Uchimura T, Towhata I, Wang L, Seko I (2008) A reliable method to monitor the time of slope failure with tilting sensors. Landslides 5(3): 325-332

Wang G, Sassa K (2003) Pore-pressure generation and movement of rainfall-induced landslides: Effects of grain size and fine-particle content. Eng Geol 69:109–125

Wong J L, Lee M L, Teo F Y, Liew K W (2022) A Review of Impacts of Climate Change on Slope Stability. Climate Change and Water Security 157-178

Xia M, Ren G M, Yang X L (2021) Mechanism of a catastrophic landslide occurred on May 12, 2019, Qinghai Province China. Landslides 18:707–720

Xiao D, Zhao X Y, Li K P, Zhao X C, Liu H W, Li X Luo G (2021) Influence of acid rain on slope instability mechanism—a case study in Sichuan provincial highway. China Bull Eng Geol Env 80(5):3659–3673

Xu Q, Zhang S, Li W van Westen C J (2021) Small-scale landslide experiments for mapping the relationship between mobility and landslide volume. Earth Surface Processes and Landforms 46(7):1514-1528

Yi X, Feng W, Bai H, Shen H Li H (2021) Catastrophic landslide triggered by persistent rainfall in Sichuan China: August 21, 2020, Zhonghaicun landslide Landslides 18:2907–2921

Zulkafli S A, Majid N A (2021) Landslides incidents in Federal Territory of Kuala Lumpur Malaysia. Ecology, Environment and Conservation 27(3):990–995

Zhang Y, Zhu Y, Yan X, Li S, Yu Q, Wang Y (2022) A determination method of rainfall type based on rainfall-induced slope instability. Natural Hazards 113(1):315–328 https://doi.org/10.1007/s11069-022-05301-2